EITを用いたレーザーの周波数差安定化（offset locking）

2013年7月24日　ランチミーティング

担当：鳥井

APPLIED PHYSICS LETTERS **90**, 171120 (2007)

Laser frequency offset locking using electromagnetically induced transparency

S. C. Bell and D. M. Heywood
Optical Physics, University of Melbourne, Victoria 3010, Australia

J. D. White
Juniata College, Huntingdon, Pennsylvania 16652

J. D. Close
Australian National University, Canberra ACT 0200, Australia

R. E. Scholten[a)]
School of Physics, University of Melbourne, Victoria 3010, Australia

(Received 20 February 2007; accepted 2 April 2007; published online 27 April 2007)

The authors have used an electromagnetically induced transparency resonance in rubidium as a dispersive reference to lock the relative frequency of two lasers to the atomic ground-state hyperfine splitting. The beat frequency between the two lasers directly generates a microwave signal at 3.036 GHz (^{85}Rb) or 6.835 GHz (^{87}Rb). High bandwidth (600 kHz) feedback was achieved with only low-frequency (10 MHz) electronics using the frequency modulation sideband method. The spectral width of the microwave beat frequency was reduced to less than 1 kHz. The technique offers a convenient and low-cost method suitable for many topical two-frequency experiments, including coherent population trapping, slow light, lasing without inversion, and Raman sideband cooling. © *2007 American Institute of Physics*. [DOI: 10.1063/1.2734471]

なぜoffset locking?

- 光の超低速伝播
- 反転分布のないレーザー発振
- 電磁誘起透明化（EIT：electromagnetically induced transparency）
- CPT（coherent population trapping）原子時計
- アルカリ原子のレーザー冷却のリポンプ光
- ラマンサイドバンド冷却
- STIRAP(stimulated Raman adiabatic passage)

3準位原子とレーザー光との相互作用

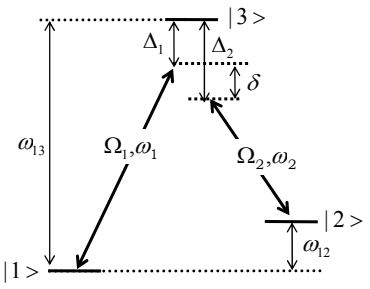

$$\hat{H} = -\delta\,|2><2| - \Delta_1\,|3><3| + \frac{\Omega_1}{2}[|1><3| + |3><1|] + \frac{\Omega_2}{2}[|2><3| + |3><2|]$$

$$|\psi> = c_1(t)\,|1> + c_2(t)\,|2> + c_3(t)\,|3>$$

$$i\hbar\frac{d}{dt}\begin{pmatrix} c_1 \\ c_2 \\ c_3 \end{pmatrix} = \frac{\hbar}{2}\begin{pmatrix} 0 & 0 & \Omega_1 \\ 0 & -2\delta & \Omega_2 \\ \Omega_1 & \Omega_2 & -2\Delta_1 \end{pmatrix}\begin{pmatrix} c_1 \\ c_2 \\ c_3 \end{pmatrix}$$

固有方程式 $$\det\begin{vmatrix} -\lambda & 0 & \Omega_1 \\ 0 & -2\delta-\lambda & \Omega_2 \\ \Omega_1 & \Omega_2 & -2\Delta_1-\lambda \end{vmatrix} = 0 \rightarrow \lambda = 0, -\Delta_1 \pm \sqrt{\Delta_1^2 + \Omega_1^2 + \Omega_2^2}$$

$$|\psi>_{\mathrm{Dark}} = \frac{1}{\sqrt{\Omega_1^2 + \Omega_2^2}}\left(\Omega_2\,|1> - \Omega_1\,|2>\right)$$

暗状態（Dark State）

3準位原子とレーザー光との相互作用

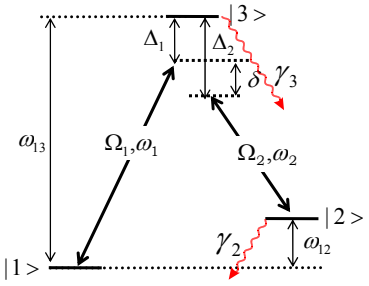

$$\Gamma_{12} = \gamma_2 - i\delta$$

$$\Gamma_{13} = \gamma_3 - i\Delta_1$$

$$\chi \propto \frac{i\Gamma_{12}}{\Gamma_{12}\Gamma_{13} + \Omega_2^2/4}$$

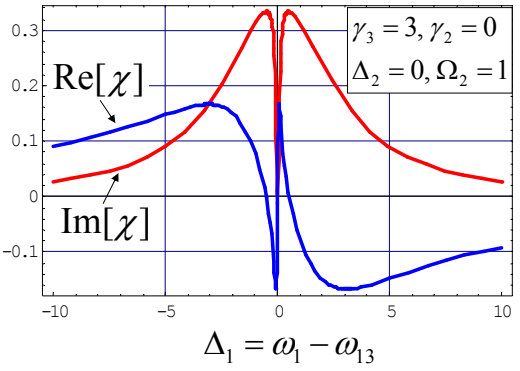

- 吸収の消失（EIT：電磁誘起透明化）
- 超低速光伝播

3振子の連成振動

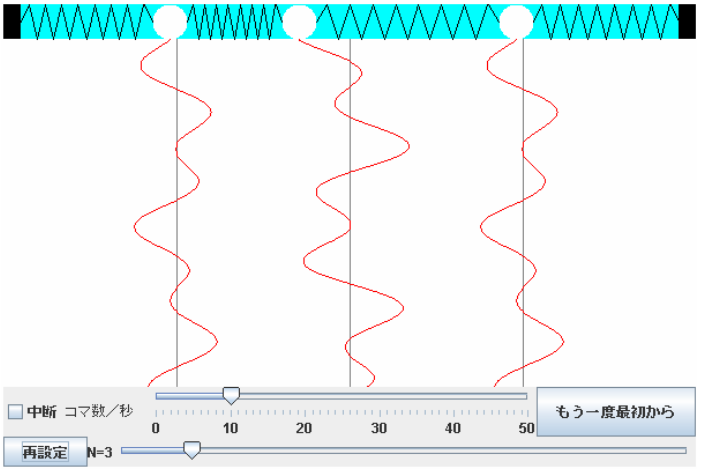

http://www.phys.u-ryukyu.ac.jp/~maeno/wave/renseiN.html

3つの固有モード

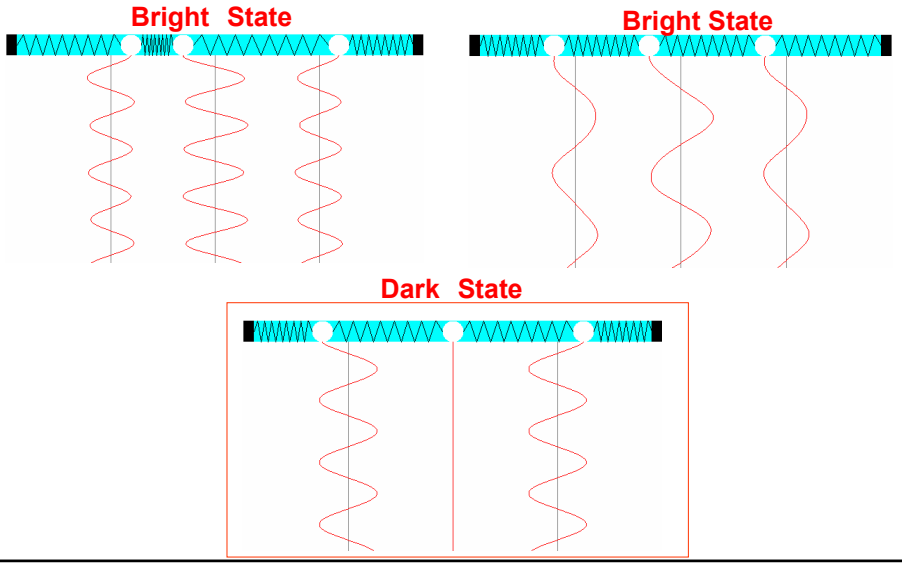

光の位相速度と群速度

$$\boldsymbol{P} = \varepsilon_0 \chi \boldsymbol{E} \quad n(\omega) = \sqrt{1+\chi(\omega)}$$

$$v_{ph} \equiv \frac{\omega}{k} = \frac{c}{n(\omega)}$$

$$v_g \equiv \frac{\partial \omega}{\partial k} = \frac{c}{n + \omega(\partial n / \partial \omega)}$$

17m/sまで光（の群速度）を減速

Light speed reduction to 17 metres per second in an ultracold atomic gas

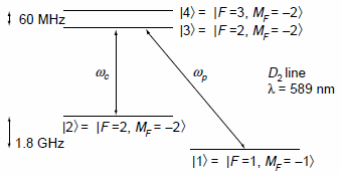

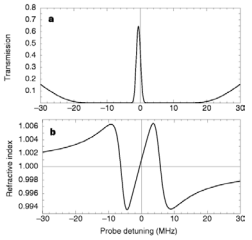

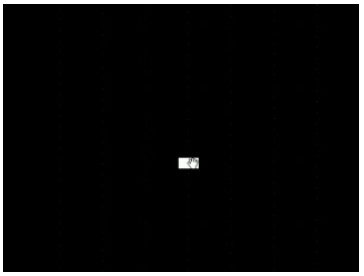

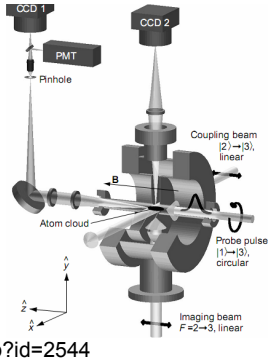

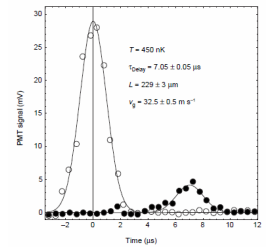

http://www.rochester.edu/news/show.php?id=2544

Nature **397**, 594(1999)

Vacuum Induced Transparency (VIT)

H. Tanji-Suzuki, W. Chen, R. Landig, J. Simon, V. Vuletic, Science **333**, 1266 (2011)

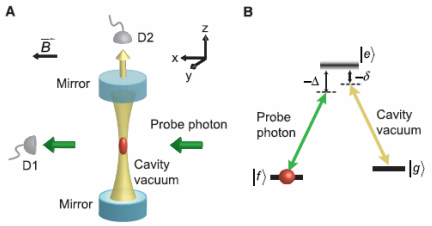

Fig. 1. (**A** and **B**) Setup (A) and atomic level scheme (B) for observing vacuum-induced transparency. An ensemble of laser-cooled ^{133}Cs atoms is trapped inside an optical cavity operating in the single-atom strong-coupling regime (cooperativity parameter $\eta > 1$). The atoms are prepared in state $|f\rangle$ by optical pumping. The absorption of a probe laser on the transition $|f\rangle \leftrightarrow |e\rangle$ is substantially altered when a cavity mode on the transition $|g\rangle \leftrightarrow |e\rangle$ is tuned near two-photon resonance. Although the cavity mode subtends only a very small ($\sim 10^{-4}$ sr) solid angle along a direction transverse to the probe beam, its vacuum field can substantially reduce the probe absorption by quantum interference. Photon counters D1 and D2 are used to measure the probe transmission and the scattering into the cavity, respectively.

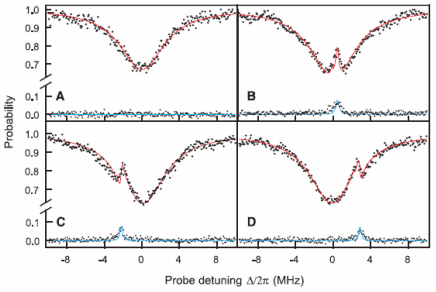

Fig. 2. (**A** to **D**) Atomic absorption spectrum (A) and VIT spectra (B to D) for different cavity-atom detunings: (B) $\delta/(2\pi) = 0.5$ MHz, (C) $\delta/(2\pi) = -2.2$ MHz, (D) $\delta/(2\pi) = 2.8$ MHz. The transmission probability (upper curves) and the probability of emission into the cavity (lower curves) are measured simultaneously versus probe-atom detuning Δ by photon-counting detectors D1 and D2. Near the two-photon resonance $\Delta \approx \delta$ the absorption is suppressed by VIT, and a fraction of the incoming photons is directed out of the cavity. Data for both processes for all values of δ are simultaneously described by the VIT model explained in the text (solid lines).

PRL 105, 013601 (2010) PHYSICAL REVIEW LETTERS week ending 2 JULY 2010

Photon-Number Selective Group Delay in Cavity Induced Transparency

Gor Nikoghosyan[1,2] and Michael Fleischhauer[1]

[1]*Department of Physics and Research Center OPTIMAS, University of Kaiserslautern, Erwin-Schrödinger-Strasse, D-67663 Kaiserslautern, Germany*

[2]*Institute of Physical Research, 378410, Ashtarak-2, Armenia*

(Received 10 October 2009; published 29 June 2010)

We show that the group velocity of a probe pulse in an ensemble of Λ-type atoms driven by a quantized cavity mode depends on the quantum state-of-the input probe pulse. In the strong-coupling regime of the atom-cavity system the probe group delay is photon-number selective. This can be used to spatially separate the single photon from higher photon-number components of a few-photon probe pulse and thus create a deterministic single-photon source.

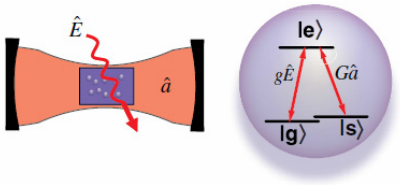

FIG. 1 (color online). Schematic diagram of the system: A quantized probe field $\hat{E}$ interacts with an ensemble of Λ-type atoms driven by a cavity mode $\hat{a}$ (left) in a Raman type coupling scheme (right).

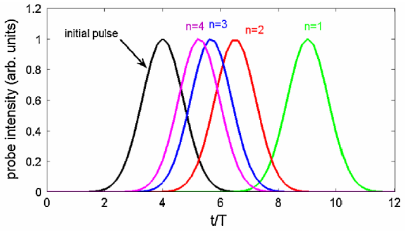

FIG. 2 (color online). Spatial separation of an initial probe pulse into Fock-state components.

feature article

The rubidium atomic clock and basic research

James Camparo

The vapor-cell atomic clock finds application today in the global positioning system and telec cations. To improve and miniaturize the humble device for future applications will require a d understanding of atomic and chemical physics.

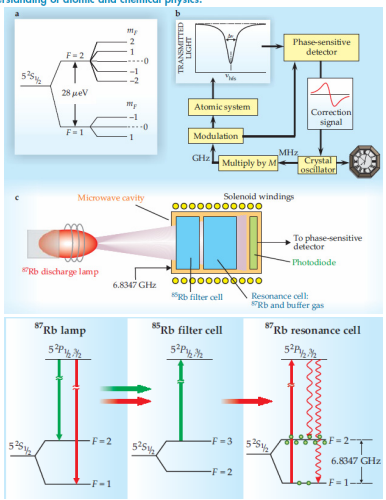

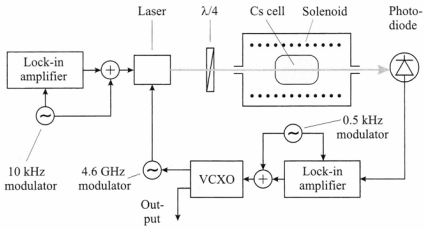

Figure 8.11: Schematic of a compact cell-based frequency reference.

Riehle, *Frequency Standards*, p253

普通のランプ式原子時計 CPT原子時計

典型的なoffset locking (OPLL)

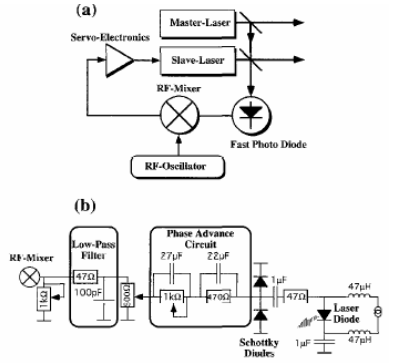

Fig. 5. (a) Schematics of the set-up for the optical phase locked loop (OPLL) between two independent lasers systems. The frequency of the master laser is stabilized to a Doppler-free resonance of the rubidium D2 line, using standard techniques. The frequency of the slave laser is stabilized by a heterodyne OPLL. (b) Electronic circuitry for the OPLL. The output signal from the RF-mixer is low-pass filtered (3 dB point at 34 MHz) to suppress the frequency of the local oscillator and its higher harmonics. A phase advance circuit then compensates for the delay with the error signal undergoes between the photodiode and the slave laser. The two Schottky diodes eliminate high frequency spikes that could damage the laser diode.

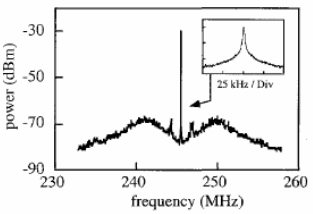

Fig. 6. Beat signal between the master laser and the slave laser with closed OPLL. A frequency span of 25 MHz was recorded with a resolution bandwidth of 1 kHz and a video filter bandwidth of 1 kHz. The increase in the noise level ±5 MHz from the center shows the noise sidebands of the stabilization loop. The inset shows a frequency span of 100 kHz, recorded with a resolution bandwidth of 1 kHz and a video filter bandwidth of 30 Hz. The width of the beat signal is limited by the resolution of the spectrum analyzer.

Opt. Commun. **117**, 541 (1995)

DBM（double balanced mixer）

動作モードその①

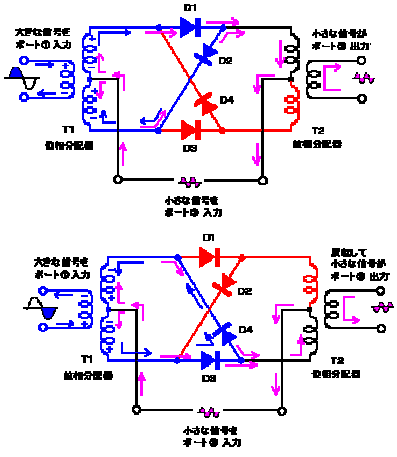

動作モードその②

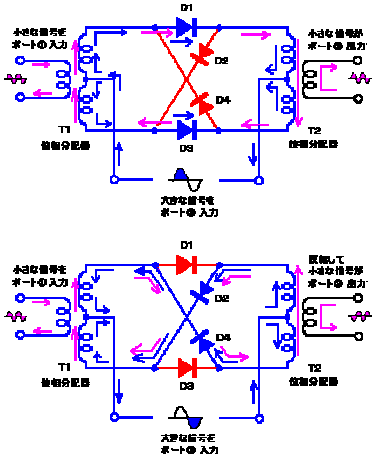

http://infoseek_rip.g.ribbon.to/spectrum123.at.infoseek.co.jp/buhin/dbm/dbm.htm

簡便なoffset locking

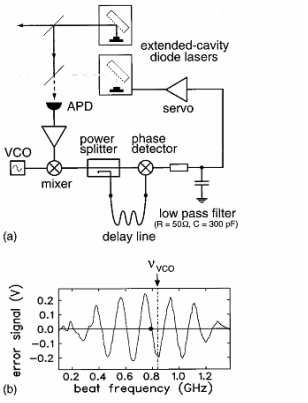

FIG. 1. (a) Scheme of the tunable frequency offset lock. (b) Error signal as a function of beat frequency between the two lasers. The dot indicates one of the locking points of the servo loop, and ν_{VCO} denotes the frequency of the rf oscillator used for frequency shifting the beat signal.

Rev. Sci. Instrum. **70**, 242 (1999)

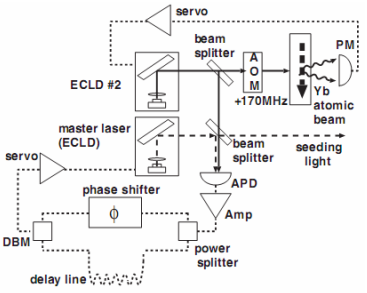

Fig. 5. Schematic diagram of absolute frequency-locking of the master ECLD. A portion (≤1 mW) of the outputs of the master ECLD and ECLD #2 was superimposed on the avalanche photodiode (APD), where frequency differences between the two lasers were detected as a beat signal. The signal was divided into two by a power splitter. One signal was phase-shifted, and the other was time-delayed. After that, they were recombined by a double-balanced mixer (DBM) and used for electrical servo-control of a piezoactuator of the master ECLD. The frequency of ECLD #2 was 170 MHz up-shifted by an acousto-optic modulator (AOM), and irradiated to the Yb atomic beam. The emission signal of Doppler-free Yb $^1S_0$–$^1P_1$ was detected by a photomultiplier tube (PMT) and used for frequency-locking.

Jpn. J. Appl. Phys. **42**, 5059 (2003)

今回の論文のセットアップ

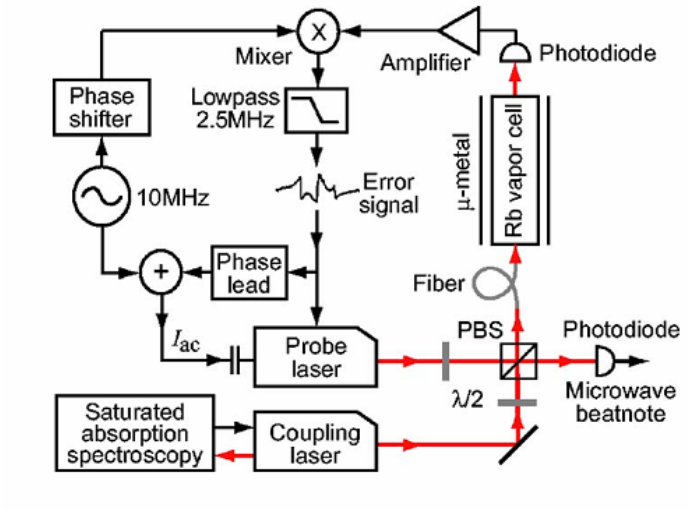

EIT信号と飽和分光信号の比較

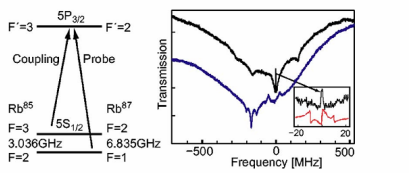

FIG. 1. (Color online) Rubidium energy levels, ^{87}Rb EIT spectrum (upper), and $F=1$ ground-state saturated absorption spectrum for probe laser (lower). The inset shows expanded EIT region with FM sideband feedback error signal. EIT peak height 30% of Doppler absorption; width of 0.85 MHz limited by linewidth of unlocked (scanning) probe laser.

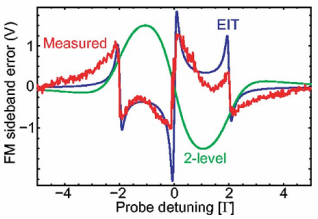

FIG. 2. (Color online) Measured FM sideband error signal for the EIT resonance compared to calculations for EIT and an equivalent two-level Doppler-free system. Opposite signs of error curves reflect sign reversal in refractive index for two- and three-level systems, calculated for strong coupling, weak probe, Rabi frequencies 2 and 0.01Γ, and modulation frequency 2Γ.

測定結果

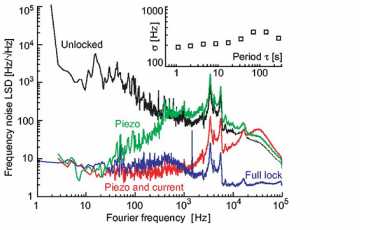

FIG. 4. (Color online) Frequency noise linear spectral density of feedback error signal; coupling laser locked, different probe laser feedback actuators enabled. Noise suppression extends to 600 kHz (not shown). Inset: overlapping Allan standard deviation $\sigma(\tau)$ of the offset beat note frequency.

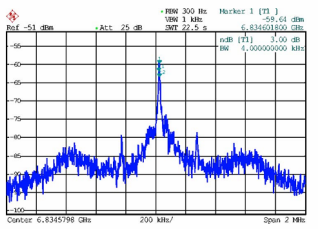

FIG. 5. (Color online) Spectrum of microwave beat note generated by interference for ^{87}Rb. −3 dB width of 4 kHz (750 Hz in 0.2 s). 200 kHz/div horizontal; 5 dB/div vertical.